Lai, D., Zhou, X., and Chen, Q. 2017. "Measurements and predictions of the skin temperature of human subjects on outdoor environments," *Energy and Buildings*, 151: 476-486.

Measurements and Predictions of the Skin Temperature of Human Subjects in Outdoor Environments

Dayi Lai[1], Xiaojie Zhou[2], Qingyan Chen[1,2,*]

[1]School of Mechanical Engineering, Purdue University, West Lafayette, IN 47907, USA
[2]Tianjin Key Lab of Indoor Air Environmental Quality Control, School of Environmental Science and Engineering, Tianjin University, Tianjin 300072, China
*Corresponding author: Qingyan Chen
Phone: +1-765-496-7562, Email: yanchen@purdue.edu

Abstract

Thermal comfort in outdoor spaces is strongly associated with the quality of social life in an urban community. This study investigated dynamic outdoor thermal comfort under cold, mild, and hot climatic conditions with air temperature ranging from -0.1 to 35.0 ºC. Using a total of 26 human subjects in 94 tests under these climatic conditions, this study measured outdoor thermal environmental parameters, monitored subjects' skin temperature, and recorded subjects' thermal sensation. The study found that fluctuations in wind speed and solar radiation led to changes in convective and radiative thermal loads on the human subjects. Their skin temperature and thermal sensation changed accordingly. In the cold conditions, the skin temperature of the trunk was stable at around 34 ºC, while the skin temperature of the face decreased to 19 ºC. This investigation developed a human heat transfer model that considers outdoor radiative heat exchange and transient heat transfer in clothing. The mean skin temperatures predicted by the model agree reasonably well with the measured data. However, the discrepancy between the predicted and measured local skin temperature under extremely cold conditions can be as large as 6 K.

Keywords: Thermal comfort; Dynamic thermal environment; Outdoor spaces; Heat transfer model

Highlights

This study investigated dynamic outdoor thermal comfort under various climatic conditions.

Fluctuations in wind speed and solar radiation lead to fluctuations in skin temperature and thermal sensation.

In cold conditions, the skin temperature difference at various body parts can be as large as 15 K.

This study developed a human heat transfer model that can predict mean skin temperature in an outdoor environment reasonably well.

1. Introduction

About 54% of the world's population lives in urban areas [1]. In cities, outdoor spaces allow citizens to exercise and socialize. A study in Japan showed that living in areas with walkable outdoor spaces increased the longevity of urban senior citizens [2]. Another study, in the Netherlands, indicated that green outdoor spaces in the living environment decreased people's feelings of aloneness [3]. In light of these physical and social benefits, it is necessary to design attractive spaces that would encourage more citizens to spend time outdoors. Among many factors that affect people's use of outdoor spaces, thermal comfort is probably the most important. A number of studies [4-8] have identified a strong correlation between outdoor thermal comfort and occupancy in outdoor spaces. For example, Lin et al. [4] demonstrated that the greatest park attendance was associated with the highest thermal comfort level.

To better understand outdoor thermal comfort, many researchers have conducted field surveys in various climate regions. For example, Nikolopoulou and Lykoudis [6] reported their findings from a large-scale study across five different European countries. The air temperature in their study ranged from 5.4 to 30.1 ^{o}C. The researchers found that 75% of the interviewees felt comfortable in outdoor spaces. Spagnolo et al. [9] investigated several open spaces in Sydney, Australia. They discovered that the outdoor neutral temperature (26.2 ^{o}C) was significantly higher than the indoor neutral temperature (24 ^{o}C). Thorsson et al. [7] studied thermal comfort in a park in an urban area in Sweden and demonstrated that

psychological aspects such as expectations, experience, and perceived control influenced the subjective thermal comfort assessment. These studies have advanced our understanding of outdoor thermal comfort. Furthermore, field surveys have revealed differences in outdoor thermal comfort among various climate regions. Aljawabra and Nikolopoulou [10] conducted case studies in hot arid areas in Marrakech, Morocco, and in Phoenix, Arizona, USA. Although the climatic conditions in the two regions were similar, most subjects in Marrakech voted for "warm," while most subjects in Phoenix voted for "hot." Nikolopoulou and Lykoudis [6] found a difference of over 10 K in neutral temperature across Europe. Lai et al. [11] found that the neutral temperature range in Tianjin, China, was different from that in Europe [12] or Taiwan [13].

The discrepancies in those studies may be due to the dynamic features of outdoor thermal comfort. Since the outdoor thermal environment can change rapidly within a short period, a person's skin and core temperatures will change accordingly but with a very significant decay. Hoppe [14] found that when a person walked from a neutral indoor environment to a cold outdoor environment of 0 ºC, his skin and core temperature reached equilibrium after 26 hours. As the skin and core temperatures of the subject decreased, his thermal sensation was likely to change. In addition, the outdoor thermal environment has large fluctuations: wind speed varies constantly, and solar radiation intensity varies with time if clouds are present. These fluctuations affect the thermal sensation of subjects. The field surveys discussed above may not have considered the thermal history of the subjects and may have recorded the thermal sensation of interviewees only at specific times. It is probable that the recorded thermal sensation had a large variation. Our literature review did not find any outdoor thermal comfort studies with a dynamic thermal history of the subjects. Therefore, it is necessary to investigate dynamic outdoor thermal comfort by considering the thermal history of subjects under a fluctuating outdoor thermal environment.

Some studies have investigated transient outdoor thermal comfort with the use of human heat transfer models. For example, Katavoutas et al. [15] employed the Institutionary Munich Energy balance Model (IMEM) to investigate the transient thermal comfort when an individual moved from an indoor to an outdoor hot environment. Their study found that skin temperature stabilized in 10 minutes, but core temperature continued to rise during the simulation. The modeling study has provided useful insights about changes in a person's thermal condition outdoors. The IMEM model in Katavoutas' study treated a human body as two nodes with uniform thermal-physical properties and clothing value for each node.

In reality, different segments of the body have different thermal-physical properties and are insulated with different clothing levels. Furthermore, the radiative heat transfer between a human body and an outdoor environment is complicated. The sun projects short-wave radiation onto each segment at different angles, and the temperatures of the surrounding objects may not be the same. The fluctuating thermal environment continuously affects the heat transfer on a human body. Hence, it is important to develop a human heat transfer model that can account for the impact of the fluctuating outdoor thermal environment and heat transfer on different parts of the human body. This paper reports our effort and results.

2. Research method

With the use of human subjects in an actual outdoor environment, the study measured outdoor thermal environmental parameters, monitored subjects' skin temperature, and recorded their thermal sensation. At the same time, a heat transfer model was developed to predict the subjects' skin temperature. The model was validated by the experimental data.

2.1. Subject tests

This investigation measured the response of human subjects to the outdoor thermal environment. Our hypothesis was that the fluctuation in the environment creates a dynamic thermal load on the human body. The changing thermal load affects the skin temperature, which determines the person's thermal sensation.

We measured thermal environmental parameters and monitored the skin temperature and thermal sensation of the subjects. To collect data from different regions, the tests were carried out in West Lafayette (WL), Indiana, USA, and Tianjin (TJ), China. The climatic conditions in the two places allow us to collect data under a wide range of thermal environments. Both cities are in "hot summer continental" climates with hot summer and cold winter. The air temperature in the summer can easily exceed 30^{o}C and the lowest air temperature in winter is below 0^{o}C. In West Lafayette, we used ten human subjects with each subject participated the tests for three to five times to yield 40 sets of data. In Tianjin 16 subjects were recruited and each of them participated the tests for three to four times, which allowed us to obtain 54 sets of data. Table 1 shows the gender and age breakdown of the subjects in Tianjin and West Lafayette. We have 19 males and 7 females participated the test. In terms of age, 20 out of the 26 subjects are younger than 30. When designing the

test, we divided the tests into seven conditions and each condition covered an air temperature range of 5 K. We obtained at least 10 sets of data for each condition. The tests in West Lafayette were conducted from March 6, 2016, to September 25, 2016 and the tests in Tianjin were from May 21, 2016, to December 14, 2016. These date ranges covered cold, mild, and hot climatic conditions.

Table 1. Numbers of subjects based on gender and age for the tests conducted in Tianjin (TJ) and West Lafayette (WL).

	Location	Male	Female	Age < 30	Age > 30	Total
Number of subjects	TJ	9	7	10	6	16
	WL	10	0	10	0	10
	Total	19	7	20	6	26

As shown in Figure 1, the subjects first stayed in a neutral indoor chamber for 30 minutes to achieve a stable thermal condition; they then moved to an outdoor space and remained there for 60 minutes. The indoor air temperature (T_a) and relative humidity (RH) were controlled at around 24 ºC and 50%, respectively. The air velocity (V_a) in the indoor chamber was kept at a minimum. The outdoor space was an open area surrounded by several low-rise buildings.

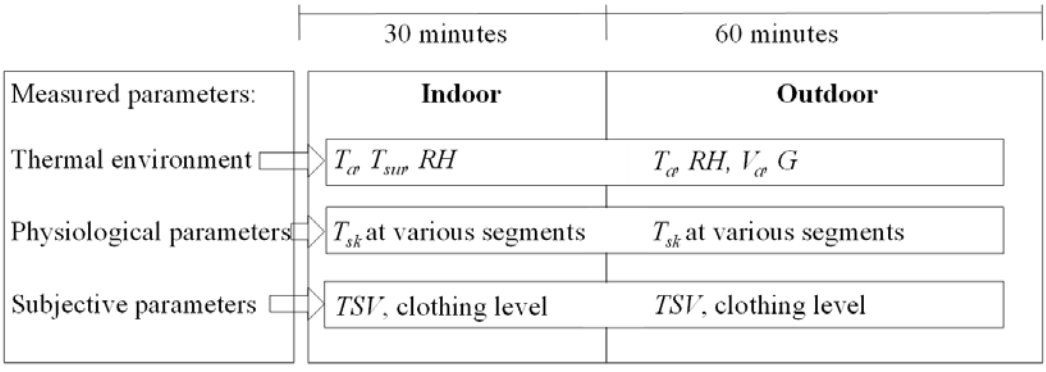

Figure 1. Measurement procedure for the human subject tests.

In the indoor chamber, T_a, RH, and surface temperature (T_{sur}) were measured. In the outdoor space, T_a, RH, V_a, and global solar radiation (G) were monitored continuously. In West Lafayette, the outdoor T_a, RH, direct solar radiation (G_{dir}), and diffuse solar radiation (G_{dif}) were monitored on the rooftop of one of the surrounding buildings. Global solar radiation G is the summation of G_{dir} and G_{dif}. Outdoor wind speed V_a was recorded every five minutes by a handheld anemometer. In Tianjin, we used a portable weather station to measure the outdoor thermal environmental parameters. Since the weather station can measure only global radiation G, we used RayMan software [16,17] to separate the global radiation into its direct and diffuse components. During the test, each subject's skin temperature (T_{sk}) at his or her head, face, thorax, abdomen, left upper arm, left lower arm, left hand, left upper leg, left lower leg, and left foot were measured continuously by thermocouples attached to these body locations as shown in Figure 2. The thermocouples were connected to portable data loggers. The response time for the thermocouple is 0.1 second. Table 2 lists the technical information for the sensors used in this study. Besides the thermal environmental parameters and skin temperatures, we obtained subjects' thermal sensation by asking them to complete the questionnaire shown in Figure 3. The questionnaire used the ASHRAE seven-point scale for thermal sensation votes (TSV). In the indoor chamber, we asked the subjects to rate their thermal sensation every ten minutes, while the outdoor thermal sensation was recorded every five minutes. We also used the questionnaire to collect data on subjects' clothing. In the indoor chamber, the subjects sat quietly, while in the outdoor space, they stood with their backs to the sun.

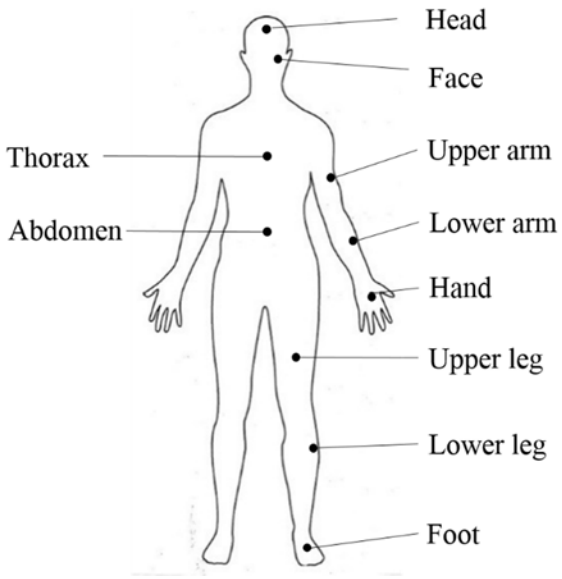

Figure 2. Monitoring locations for skin temperature.

Table 2. Sensors used to measure thermal environmental parameters and skin temperature.

Parameter	**Sensor**	**Range**	**Accuracy**	**Interval**
T_a, indoor	HOBO U12	-20 to 70 °C	±0.35 K from 0 to 50 °C	1 min.
RH, indoor	HOBO U12	5 to 95%	±2.5% from 10 to 90%	1 min.
T_{sur}	D501	-45 to 287 °C	±2%	10 min.
T_a, outdoor	S-THB-M002	-40 to 75 °C	±0.2 K at 20 °C	1 min.
RH, outdoor	S-THB-M002	0 to 100%	±3%	1 min.
V_a, WL	WM4	0.35 to 40 m/s	±3%	5 min.
G_{dir}, G_{dif}, WL	SPN1	0 to > 2000 W/m^2	±5% ± 10 W/m^2	5 min.
V_a, TJ	S-WSET-A	0–45 m/s	±1.1 m/s	1 min.
G, TJ	S-LIB-M003	0-1280 W/m^2	±10 W/m^2 or ±5%	1 min.
T_{sk}	TT-K-30-SLE	0 to 350 °C	±1.1 °C or ±0.4%	1 sec.

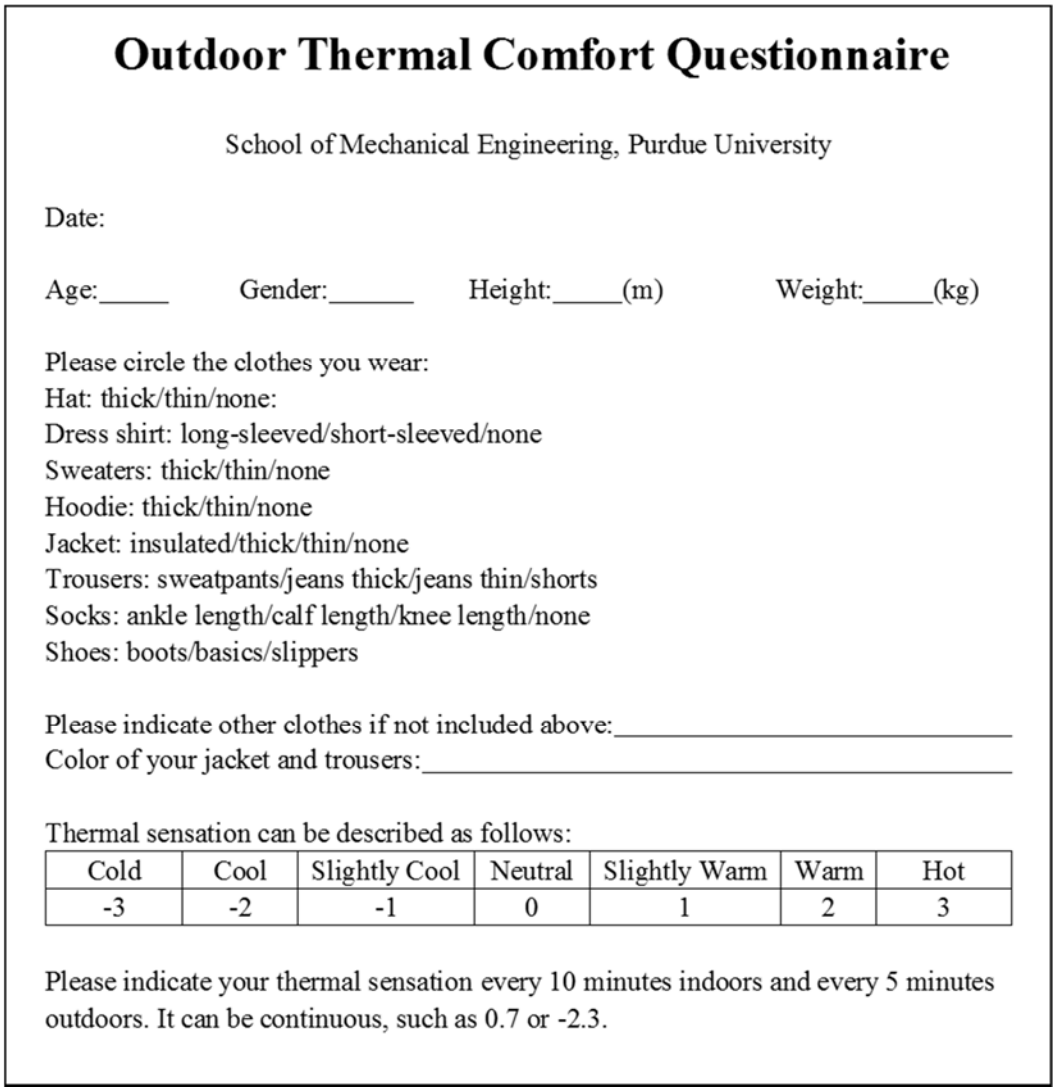

Outdoor Thermal Comfort Questionnaire

School of Mechanical Engineering, Purdue University

Date:

Age:_____ Gender:_____ Height:_____(m) Weight:_____(kg)

Please circle the clothes you wear:
Hat: thick/thin/none:
Dress shirt: long-sleeved/short-sleeved/none
Sweaters: thick/thin/none
Hoodie: thick/thin/none
Jacket: insulated/thick/thin/none
Trousers: sweatpants/jeans thick/jeans thin/shorts
Socks: ankle length/calf length/knee length/none
Shoes: boots/basics/slippers

Please indicate other clothes if not included above:_____
Color of your jacket and trousers:_____

Thermal sensation can be described as follows:

Cold	Cool	Slightly Cool	Neutral	Slightly Warm	Warm	Hot
-3	-2	-1	0	1	2	3

Please indicate your thermal sensation every 10 minutes indoors and every 5 minutes outdoors. It can be continuous, such as 0.7 or -2.3.

Figure 3. Questionnaire used in this study.

2.2. Definition of outdoor climatic conditions

We used the universal thermal climate index (*UTCI*) [18] to classify our tests. The index assesses the outdoor thermal environment by integrating the effects of air temperature, humidity, radiation, and wind. In our study, *UTCI* was calculated by a program provided on the www.utci.org website. According to the *UTCI* stress categories [18], we defined those tests with *UTCI* values between 9 and 26 ^{o}C as mild, those with values lower than 9 ^{o}C as cold, and those with values above 26 ^{o}C as hot. On the basis of this categorization, we conducted six cold tests, eight mild tests, and six hot tests in West Lafayette, and six cold tests, six mild tests, and seven hot tests in Tianjin.

In order to examine the fluctuation of the outdoor thermal environmental parameters, we defined a fluctuation index (*FI*):

$$FI = \sigma / \mu \quad (1)$$

where σ is the standard deviation of the measured thermal environmental parameter and μ the mean value of that parameter. A higher *FI* indicates a larger fluctuation.

2.3. Human heat transfer model

To determine the thermal comfort level, a heat transfer model for a human body is needed. By improving our two-dimensional model for calculating heat transfer in the human body in a transient and non-uniform thermal environment [19], this study developed a new model that addresses the outdoor radiative heat transfer and transient heat transfer in clothing. This section presents the details of the new model.

Our original heat transfer model divided the human body into 12 segments: the head, face, neck, shoulders, thorax, abdomen, upper arms, lower arms, hands, upper legs, lower legs, and feet. The heat transfer between the body segments was conducted by blood circulation. The model allowed non-uniform clothing insulation on each segment. Inside the body, two-dimensional heat transfer along the radial and angular directions was considered in different body segments. Outside the body, at the boundary, the heat transfer included convective, radiative, and evaporative heat exchange on the skin and clothing surfaces. Besides the passive heat transfer, the model used an active system that controls the thermoregulation process within the human body. When the human body deviates from neutral state, the active system of the model will change the levels of heat production by shivering, evaporative heat exchange by sweating, and blood flow by vasomotion. The model was able to deal with sudden changes in thermal environment, sun position, clothing value, activity level, and posture.

2.3.1. Radiation model

Heat transfer on a human body in an outdoor space is significantly different from that indoors. Figure 4 shows the various forms of heat transfer between a human body and the outdoor environment. Convection, evaporation, and respiration can be calculated by the

methods described by Lai and Chen [19]. The main difference between indoor and outdoor human body heat transfer is radiation. The outdoor radiation field includes direct and diffuse short-wave radiation from the sun, and long-wave radiation from the sky and from solid surfaces such as building façades and the ground.

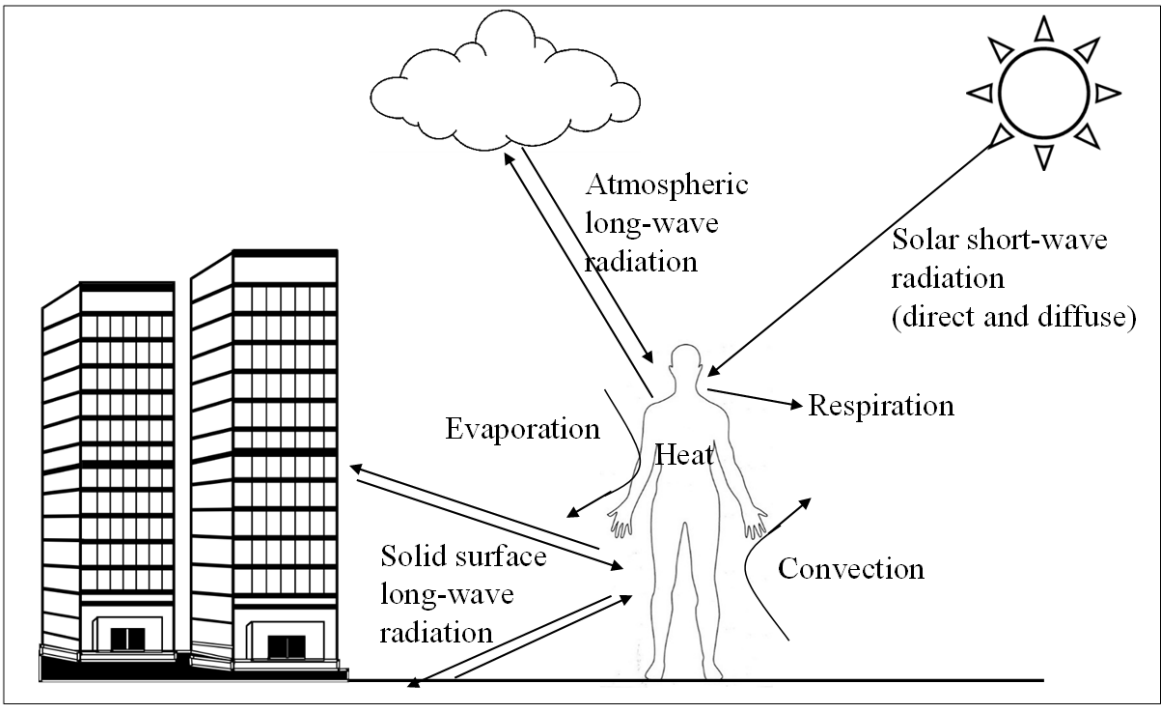

Figure 4. Heat transfer between a human body and the outdoor environment.

The rate of short-wave radiative heat gain R_S is the summation of the direct solar radiative heat gain (R_{dir}) and the diffuse solar radiative heat gain (R_{dif}). They are calculated as:

$$R_{dir} = \alpha f_{p,dir} G_{dir} \tag{2}$$

$$R_{dif} = \alpha f_{p,dif} G_{dif} \tag{3}$$

where α is the short-wave absorptivity of the human body surface, and $f_{p,dir}$ and $f_{p,dif}$ are the projected area factors for direct and diffuse short-wave radiation, respectively. The projected area factors denote the percentages of the surface exposed to the corresponding

types of radiation. The values of $f_{p,dir}$ and $f_{p,dif}$ are estimated by a method developed by Kubaha et al. [20]. They correlated $f_{p,dir}$ with the solar altitude and azimuth angle, and $f_{p,dif}$ with the ground albedo for different segments of the human body in standing and sedentary positions.

The long-wave radiation indoors is from the room surfaces, whose temperature is similar to the air temperature in the room. In an outdoor space, however, the temperatures of surfaces such as the sky and solid structures are different from the outdoor air temperature. In our study, we defined a long-wave radiant temperature (T_{lr}) for an imaginary outdoor enclosure so that the long-wave radiant heat transfer from a human body to this enclosure is equal to the actual long-wave radiant heat transfer from the human body to the actual outdoor space. T_{lr} is calculated by combining the atmospheric radiation from the sky (R_{at}) and the long-wave radiation from solid surfaces (R_{so}):

$$\varepsilon_{sur}\sigma T_{lr}^4 = (1-0.5\cdot SVF)\cdot R_{so} + 0.5\cdot SVF\cdot R_{at} \tag{4}$$

where $\sigma = 5.67\times10^{-8}$ W/m^2/K is the Stefan-Bolzmann constant, ε_{sur} the emissivity of the surroundings, and *SVF* the Sky View Factor [21]. We used the Angstrom formula [22] to calculate the atmospheric radiation R_{at}:

$$R_{at} = \sigma\cdot T_a^4\cdot(0.82-0.25\cdot10^{-0.0945\cdot V_P})\cdot(1+0.21\cdot(\frac{N}{8})^{2.5}) \tag{5}$$

where T_a is the air temperature (K), V_P the water vapor pressure (hPa), and N the degree of cloud cover, which ranges from zero to eight. The long-wave radiation from solid surfaces R_{so} is the combination of emitted radiation from a solid surface with temperature T_{so} (K) and reflected atmospheric radiation:

$$R_{so} = \varepsilon_{sur}\sigma T_{so}^4 + (1-\varepsilon_{sur})\cdot R_{at} \tag{6}$$

The surface temperature T_{so} can be iteratively determined via a method used by Matzarakis et al. [16]. With the long-wave radiation temperature T_{lr}, the rate of the long-wave radiative heat exchange R_L becomes:

$$R_L = f_{cl}h_{lr}(T_{lr}-T_{sf}) \tag{7}$$

where f_{cl} is the clothing area factor that accounts for the increased area due to clothing and T_{sf} the human surface temperature (K). If there is no clothing on the body segment, T_{sf} is

the skin temperature T_{sk}. Otherwise, T_{sf} is the same as the clothing temperature T_{cl}. The h_{lr} is the long-wave radiative heat transfer coefficient (W/m^2/K) and is defined by the Stefan-Bolzmann law:

$$h_{lr} = \sigma \varepsilon_{sf} \varepsilon_{sur} \psi_{sf-sur} (T_{sf}^2 + T_{rl}^2)(T_{sf} + T_{rl}) \quad (8)$$

where ε_{sf} is the emissivity of a human body surface and $\Psi_{sf\text{-}sr}$ the view factor between the body surface and the surrounding environment.

2.3.2. Transient clothing heat transfer model

The clothing temperature T_{cl} is needed for the calculation of long-wave radiation. Since the heat transfer on the outdoor human body is dynamic, we established a transient energy balance equation for various body parts to solve for the T_{cl} at different segments:

$$m_{cl} c_{cl} \frac{dT_{cl}}{dt} = A_{cl} \frac{T_{sk} - T_{cl}}{I_{cl}} + R_S - A_{cl} h_c (T_{cl} - T_a) - A_{cl} h_{lr} (T_{cl} - T_{lr}) \quad (9)$$

where m_{cl} is the clothing mass (kg), c_{cl} the clothing heat capacity (kJ/kg/K), A_{cl} the clothing surface area (m^2), h_c the convective heat transfer coefficient (W/m^2/K), and I_{cl} the clothing thermal resistance (m^{2}K/W). This equation shows that a clothing element gains heat from the skin and the sun and loses heat to the surroundings by convection and long-wave radiation. The left-hand term of Eq. (9) is the net heat gain, which affects the clothing temperature.

2.3.3. Thermal load calculation

Thermal load (*TL*) is the difference between the heat gain and heat loss of a human body when the skin temperature is maintained at a neutral level and sweating is kept at a minimum. With the aid of the above human heat transfer model, the thermal load of a human body in the outdoor environment is calculated as:

$$TL = (M - W + R_S) - (C + R_L + E_{sk} + C_{res} + E_{res}) \quad (10)$$

where M is the rate of metabolic heat production (W/m^2), W the rate of mechanical work (W/m^2), C the rate of convective heat loss (W/m^2), E_{sk} the rate of evaporative heat loss

from the skin (W/m^2), and C_{res} and E_{res} are the rates of convective and evaporative heat loss, respectively, via respiration (W/m^2).

3. Results

This section first reports the measured outdoor thermal environmental parameters, the skin temperatures of the human subjects under these environmental conditions, and the thermal sensation recorded by the subjects. The performance of the model in predicting the skin temperatures of the subjects is then compared with the corresponding experimental data.

3.1.Outdoor thermal environment

Table 3 summarizes the measured mean, maximum, and minimum air temperature T_a, relative humidity *RH*, wind speed V_a, and global radiation *G* (summation of G_{dir} and G_{dif}) for the cold, mild, and hot conditions during the subject tests in West Lafayette and Tianjin. The air temperature ranged from -0.1 to 35.0 ^{o}C. The measured wind speed in Tianjin was lower than that in West Lafayette. Because of the frequent smog in Tianjin, the global radiation in that city under the mild and cold conditions was much lower than that in West Lafayette. The climatic conditions during the tests correspond to the typical outdoor thermal environment in the two places.

Table 3. The measured mean, maximum, and minimum air temperature T_a, relative humidity *RH*, wind speed V_a, and global radiation *G* for cold, mild, and hot conditions during the subject tests.

		T_a (^{o}C)	*RH* (%)	V_a (m/s)	*G* (W/m^2)
WL-Cold	Average	5.7	60.2	1.9	367.2
	Max.	11.9	82.1	2.9	622.7
	Min.	-1.0	42.0	1.5	172.4
WL-Mild	Average	12.4	60.8	1.3	476.8
	Max.	22.0	86.9	2.4	858.2

	Min.	7.2	40.9	1.0	132.0
WL-Hot	Average	27.0	50.9	1.2	593.2
	Max.	33.8	65.2	2.3	960.1
	Min.	19.2	38.4	0.4	355.0
TJ-Cold	Average	7.1	55.0	0.7	169.1
	Max.	11.0	89.3	0.9	451.2
	Min.	1.9	21.0	0.5	18.7
TJ-Mild	Average	15.2	59.6	1.8	226.8
	Max.	22.3	67.8	2.0	357.1
	Min.	13.8	44.5	0.3	50.9
TJ-Hot	Average	29.6	40.4	0.7	502.6
	Max.	35.0	62.2	1.3	904.2
	Min.	24.8	24.9	0.2	59.7

The *FI* for air temperature was 0.051, relative humidity 0.022, wind speed 0.498, and global radiation 0.188, as calculated from the measured data. The outdoor wind speed exhibited the highest fluctuations, followed by the global solar radiation because some of the measurements were carried out under partially cloudy conditions. Dynamic environmental stimulation is one of the reasons that people go outdoors [23]. The fluctuations in environmental parameters and the wide range of thermal conditions make the outdoor thermal environment different from the indoor environment. These differences lead to changes in skin temperature, as shown in the following section.

3.2.Mean skin temperature of the human subjects

For the above outdoor conditions, Figure 5(a) shows the measured mean skin temperature $T_{sk,m}$ of the subjects in all cold tests in West Lafayette and Tianjin. The $T_{sk,m}$ of the subjects was between 33 and 34 ^{o}C before their stay in the cold environment. During the time that they spent outdoors, the $T_{sk,m}$ of the subjects decayed exponentially. At the end of the tests, their $T_{sk,m}$ ranged from 28.5 to 31 ^{o}C and was still decreasing. It is noteworthy that subjects' skin temperatures in the West Lafayette tests was generally lower than that in the Tianjin tests. The difference occurred because West Lafayette had lower air

temperature and higher wind speed than Tianjin during the tests.

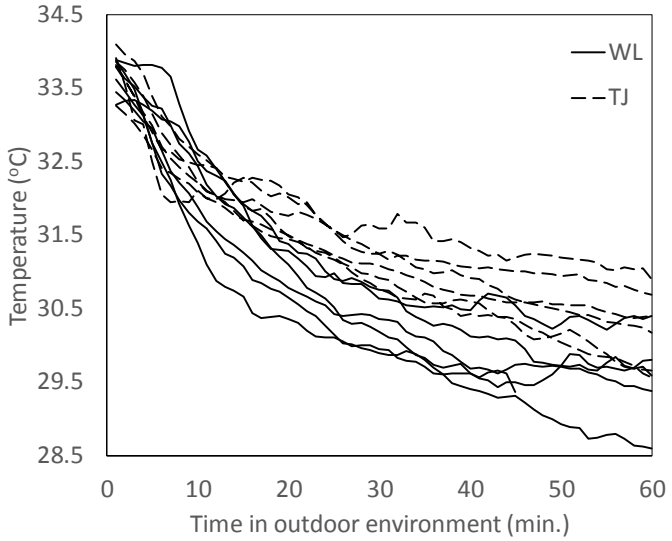

(a)

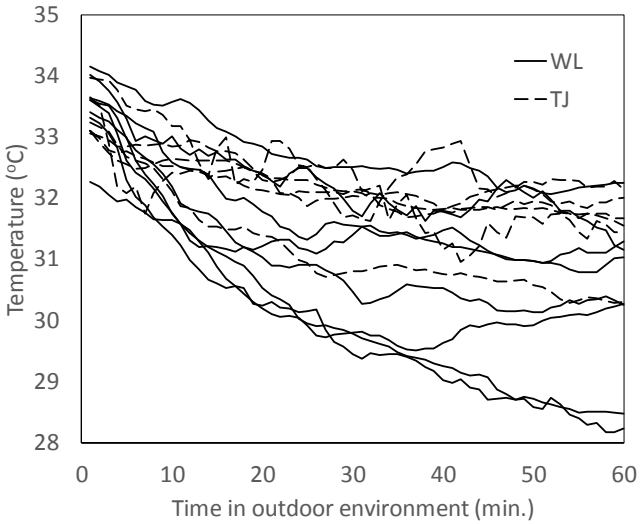

(b)

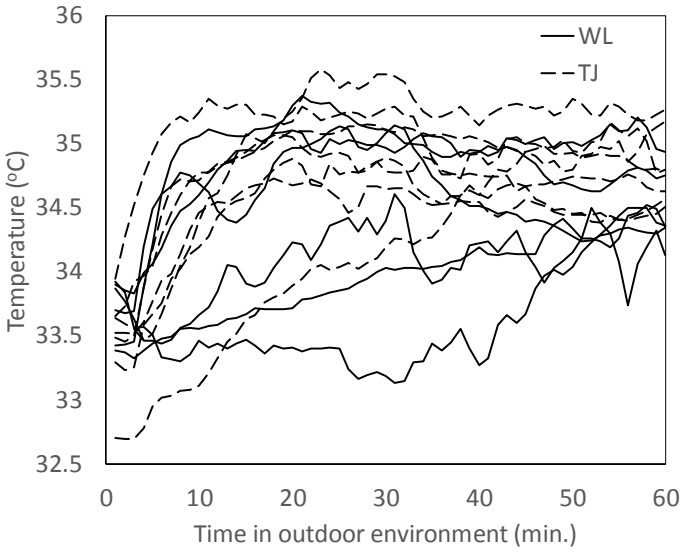

(c)

Figure 5. Measured $T_{sk,m}$ of subjects in outdoor spaces in West Lafayette and Tianjin during (a) cold tests, (b) mild tests, and (c) hot tests.

For the mild tests, Figure 5(b) shows that the $T_{sk,m}$ decreased, but the magnitude of the reduction was smaller than that in the cold cases. The final $T_{sk,m}$ was between 30.3 and 32.2 °C except for two tests, during which the subjects wore shorts when the outdoor air temperature was low, at around 12 °C. For most of the mild tests, the $T_{sk,m}$ stabilized in the end, although some minor fluctuations existed.

Figure 5(c) depicts the $T_{sk,m}$ of subjects in the hot cases. Unlike the skin temperature in the cold and mild tests, the $T_{sk,m}$ in the hot tests increased. At the end of the tests, the $T_{sk,m}$ ranged between 34.1 and 35.3 °C. For most of the tests, the temperature stabilized within 20 minutes.

It is also interesting to compare Figures 5(a), (b), and (c). In the cold conditions, the maximum decrease in $T_{sk,m}$ was more than 5 K, and the skin temperature was still decreasing after one hour. However, in the hot conditions, the maximum increase in $T_{sk,m}$ was only 2 K, and the skin temperature stabilized within 20 minute. In the cold conditions, the air temperature was much lower than the skin temperature, but in the hot conditions, the highest air temperature was only a few degrees higher than the skin temperature. Thus, the large difference between the air and skin temperatures for the cold conditions was the driving force for the decrease in $T_{sk,m}$.

As can be concluded from Figure 5, skin temperature was closely related to the thermal environmental parameters. The skin temperature levels measured outdoors generally deviated from the indoor neutral level of 33.5 ºC [24] because of the broad ranges of the thermal environmental parameters and the correspondingly large changes in heat transfer.

3.3.Thermal load of a human body in its surroundings

For an in-depth and clear understanding of the skin temperature under different outdoor conditions, this investigation selected a typical case from each stress category for detailed thermal load analysis. The typical cases are representative of the $T_{sk,m}$ within their categories. Table 4 shows the thermal environmental parameters together with their standard deviations for the three cases selected. From the standard deviation , we can see that the cold case had the highest fluctuation. The thermal environment of the hot case was the most stable within the three cases.

Table 4. Thermal environmental conditions together with their standard deviations for the three typical cases.

	T_a (ºC)	RH (%)	V_a (m/s)	G (W/m^2)	$UTCI$ (ºC)
Cold	0.8 (0.3)	54.1 (3.8)	1.4 (0.7)	622.7 (38.7)	2.3 (6.0)
Mild	22.3 (0.2)	44.5 (1.1)	1.0 (0.6)	357.1 (59.9)	24.7 (2.0)
Hot	33.3 (0.5)	55.6 (1.0)	0.3 (0.3)	264.9 (32.0)	36.8 (1.9)

As shown in Figure 4, the human body is subjected to different forms of heat transfer in the outdoor environment. By using the human heat transfer model described in Section 2.4, we estimated the thermal loads during the subjects' exposure to the outdoor environment for the cases shown in Table 4. The primary thermal loads were convection (C), short-wave radiation (R_S), long-wave radiation (R_L), metabolic heat production (M), and evaporation (E). The thermal loads were determined by using the neutral skin temperatures of different segments as listed in Table 5. In this table we have compared the indoor neutral skin temperature measured in this study and that measured by Olesen [24]. The mean skin temperature was obtained by weighting the skin temperature at different segments. We used the weighting coefficients adopted by Fiala [25]. It can be seen in the table that our measured indoor neutral temperatures agreed well with those from Olesen, which confirms the accuracy of our measurements.

Table 5. The means and standard deviations of the neutral skin temperatures of different body segments measured in this study and by Olesen [24].

Locations	**This study**	**Olesen [24]**
Mean skin	33.6 ± 0.5	33.5 ± 0.5
Head	34.3 ± 0.5	34.2 ± 1.0
Face	32.8 ± 0.8	NA
Thorax	34.8 ± 0.7	34.4 ± 0.6
Abdomen	35.0 ± 0.9	34.9 ± 1.0
Upper arm	32.8 ± 1.1	33.5 ± 0.9
Lower arm	33.3 ± 1.1	32.7 ± 0.8
Hand	33.5 ± 1.5	33.5 ± 1.0
Upper leg	32.4 ± 1.1	33.7 ± 0.8
Lower leg	32.1 ± 1.0	32.6 ± 1.1
Foot	33.8 ± 1.6	32.2 ± 2.0

Figure 6(a) shows the change in thermal load with time for a human subject in the outdoor environment in the cold case. The metabolic heat gain M was constant at 70 W/m^2. The heat gain from short-wave radiation (R_S) was 69 W/m^2. The R_S increased slightly during the test because the test was carried out in the morning and the solar radiation increased over time. The greatest heat loss was from convection because of the low air temperature and high wind speed. The convective heat loss varied from 67 to 211 W/m^2 because of the fluctuation in wind velocity. The wind fluctuation also affected the clothing temperature and the surrounding surface temperatures, and thus produced significant changes in long-wave radiation R_L. The heat loss from evaporation was only 20 W/m^2, which was much smaller than the other forms of thermal load. Because of the great variation in convective heat loss, the total thermal load ranged from -32 to -157 W/m^2.

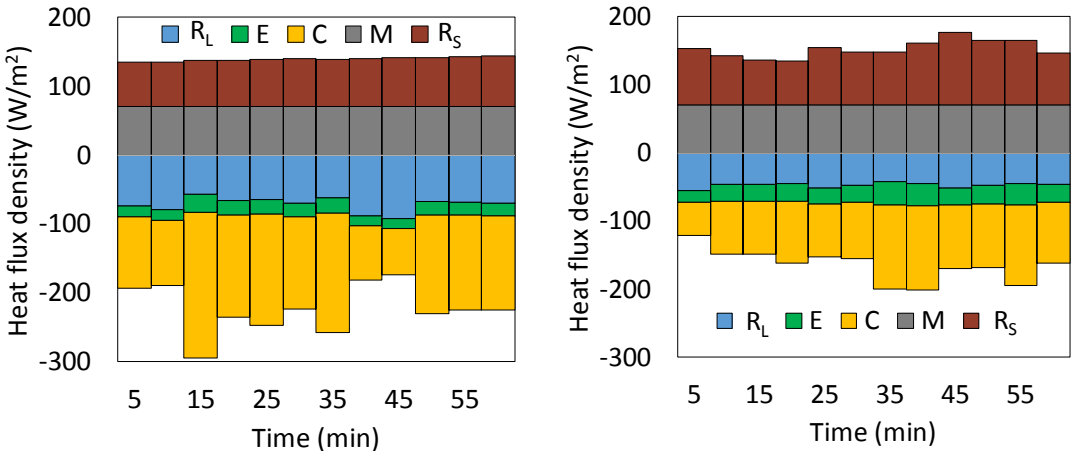

(a) (b)

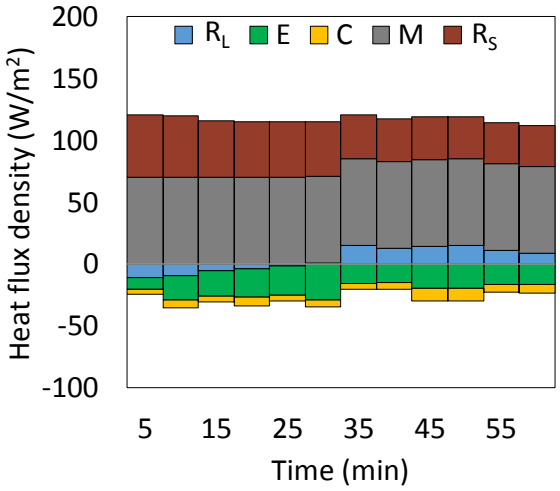

(c)

Figure 6. Changes in various forms of thermal load for an individual in the outdoor environment: (a) cold case, (b) mild case, and (c) hot case.

In the mild case, as shown in Figure 6(b), the *Rs* heat gain varied from 64 to 106 W/m^2 because direct solar radiation was frequently blocked by clouds. The convective heat loss ranged from 49 to 124 W/m^2. The temperature difference between the human surface and the air in the mild case was smaller than the difference in the cold case. As a result, the convective heat loss in the mild case was less than that in the cold case. The heat gain for the individual in the mild case was almost balanced by the heat loss. The net thermal load

ranged from -31 to 39 W/m^2.

In the hot case, as depicted in Figure 6(c), the net thermal load still reached an average value of 90 W/m^2 because of the small convective heat loss, even though the average short-wave radiative thermal load was only 41 W/m^2. The convective heat loss was small because of the low air speed and the very small temperature difference between the human body surface and the air.

The thermal load magnitudes for the three cases differed significantly from each other. For example, the averaged total thermal loads were -83, -13, and 90 W/m^2 for the cold, mild, and hot cases, respectively. The differences arose mainly from the convection due to the various temperature differences between the human body surface and the air. The mean convective heat losses were 132, 91, and 6 W/m^2 for the cold, mild, and hot cases, respectively. These differences caused the variations in the skin temperatures, as shown in the next section.

3.4. Model performance in predicting the mean skin temperature

The measured mean skin temperatures ($T_{sk,m}$) can be used to assess the model's calculation of $T_{sk,m}$. Figure 7(a) compares the measured and calculated $T_{sk,m}$ for the subjects under dynamic outdoor thermal conditions indicated by UTCI. The error bars of the measured $T_{sk,m}$ are the standard deviations of the $T_{sk,m}$ for different subjects. It can be seen that the measured $T_{sk,m}$ continued to decrease for the first 30 minutes. The rate of decrease was high at first, but it gradually slowed down. For the next 30 minutes, because of the change in wind speed and the corresponding convective heat transfer, the measured $T_{sk,m}$ showed minor fluctuations of ±0.3 K. The change in the wind speed is reflected in the change in the UTCI. At the end of the exposure period, the $T_{sk,m}$ was 30.4 ^{o}C. The model was capable of predicting the decrease and the fluctuations in $T_{sk,m}$. However, because the five-minute recording interval for wind speed and solar radiation was not sufficient to capture all the changes, the model failed to predict some of the minor fluctuations in $T_{sk,m}$.

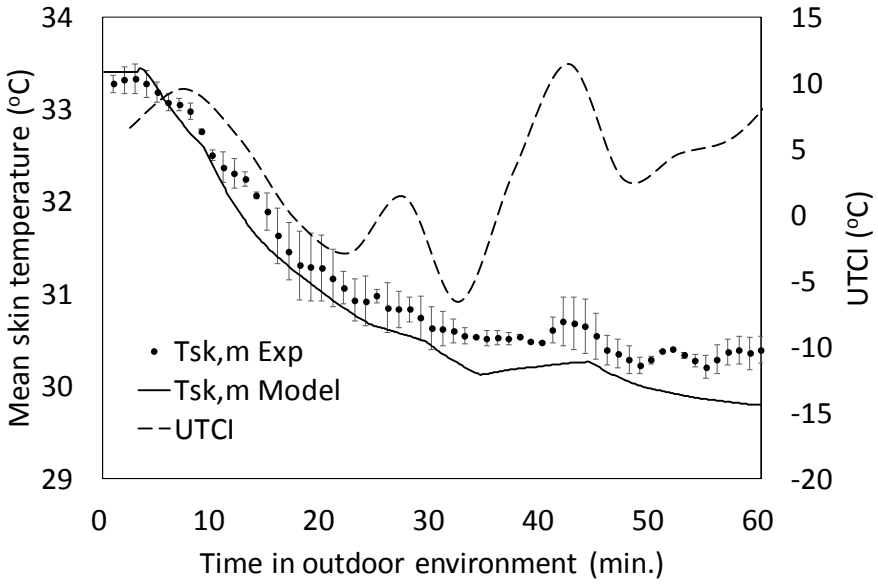
Mean skin temperature (°C)
UTCI (°C)
Time in outdoor environment (min.)
Tsk,m Exp
Tsk,m Model
UTCI
34
33
32
31
30
29
15
10
5
0
-5
-10
-15
-20
0
10
20
30
40
50
60

(a)

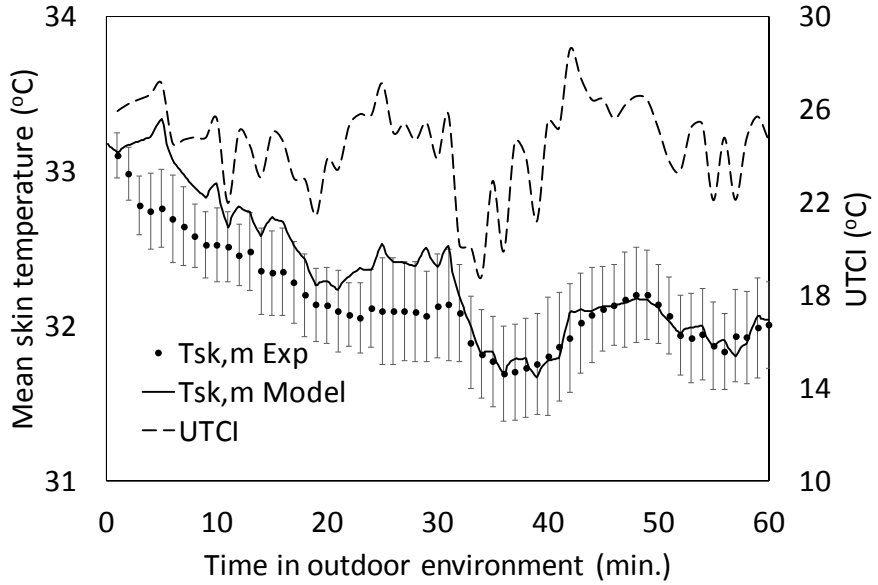
Mean skin temperature (°C)
UTCI (°C)
Time in outdoor environment (min.)
Tsk,m Exp
Tsk,m Model
UTCI
34
33
32
31
30
26
22
18
14
10
0
10
20
30
40
50
60

(b)

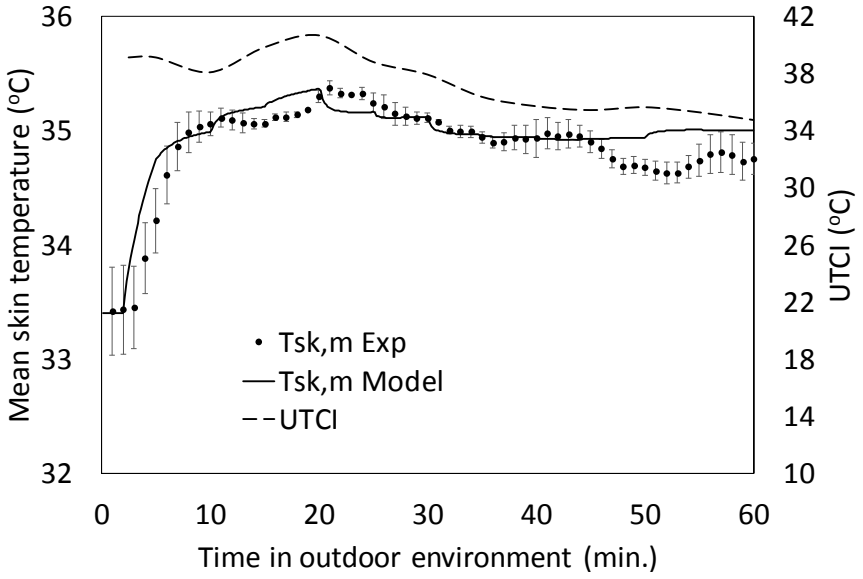

(c)

Figure 7. Measured and calculated $T_{sk,m}$ for subjects under dynamic outdoor climatic conditions indicated by UTCI: (a) cold case, (b) mild case, and (c) hot case.

Figure 7(b) compares the measured and calculated $T_{sk,m}$ for the mild-climate test in Tianjin. The measured $T_{sk,m}$ had an overall decreasing trend. At t = 35 minutes, because the elevated wind speed reduced the UTCI, $T_{sk,m}$ was decreased by 0.4 K. At t = 45 minutes, $T_{sk,m}$ returned to the previous level as the wind speed dropped and the solar radiation increased. At t = 55 minutes, the local minimum of $T_{sk,m}$ corresponded to the increase of wind. When the test was finished, $T_{sk,m}$ was 32.1 °C. The change in the mean skin temperature generally corresponds to the changes in UTCI. With the one-minute recording frequency for wind speed and solar radiation in Tianjin, the prediction accurately captured the variation in $T_{sk,m}$ during the second half hour. During the first half hour, the prediction showed a large number of small fluctuations in $T_{sk,m}$. This occurred because the wind speed measured during that period had many abrupt changes.

Figure 7(c) provides a comparison of the measured and calculated $T_{sk,m}$ for the hot-climate test in West Lafayette. The measured $T_{sk,m}$ increased to 35.3 °C at t = 20 minutes. The clothing absorbed sweat from the subject, and as the sweat penetrated the clothing, evaporation started to increase and $T_{sk,m}$ began to decrease. At the end of the test, $T_{sk,m}$ was 34.7 °C. The prediction of $T_{sk,m}$ was generally acceptable, except that it missed the fluctuation at the end of the test, which led to an error of 0.4 K.

Unlike $T_{sk,m}$ in the indoor environments, the $T_{sk,m}$ values in the outdoor spaces usually

deviated from the neutral value of 33.5 °C and changed dynamically. During the three tests, the mean skin temperature of the subjects ranged from 30.4 to 35.3 °C. The cold-climate case had the most significant overall change in $T_{sk,m}$, but the fluctuation in $T_{sk,m}$ was minor because of the heavy clothing insulation. Compared to the cold case, the mild case had a smaller overall change in $T_{sk,m}$. However, in the mild case, where the average clothing value of subjects was only 0.47 clo, the skin temperature changed immediately with the thermal environment. In the hot case, because the thermal environment was stable, $T_{sk,m}$ was also stable.

The model's predictions of $T_{sk,m}$ for the three selected tests were satisfactory. Figure 8 compares the measured and calculated $T_{sk,m}$ for all the tests. The results show that in 94.7% of the cases, there was a difference of less than 1 K between the predicted and measured $T_{sk,m}$; in 74.9% of the cases, the difference was less than 0.5 *K*. Many factors contributed to these differences. For example, the thermal and physiological properties of the human body in the model may have been different from the actual properties of the subjects. The clothing resistance values used in the prediction were estimated from tabulated values. The recording frequency of wind speed and solar radiation was not high enough to capture all the dynamic changes in the thermal environment. With these uncertainties, the performance of the model in predicting the mean skin temperature is acceptable.

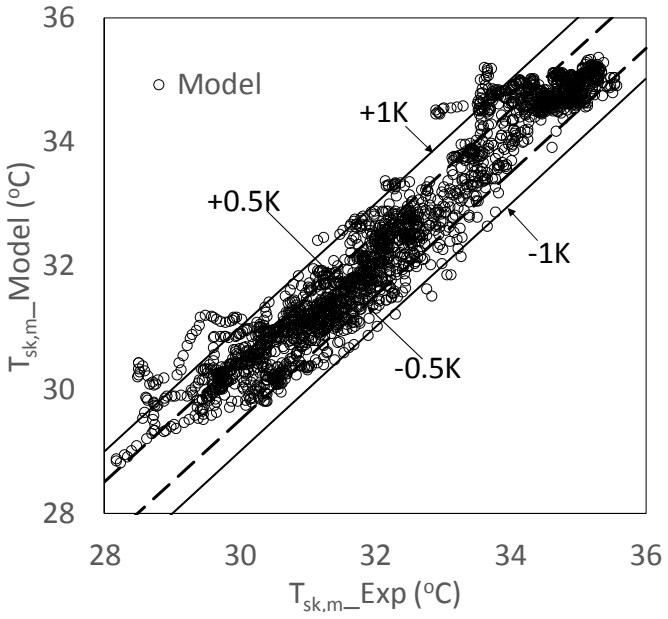

Figure 8. Comparison between the measured and predicted $T_{sk,m}$ for all the cases.

3.5.Mean skin temperature and thermal sensation

The mean skin temperature is correlated with the thermal sensation of the subjects. Figure 9 depicts the measured $T_{sk,m}$ and the *TSV* reported by the subjects in the outdoor spaces in the three typical cases. It can be seen that the *TSV* generally followed $T_{sk,m}$. For example, in the cold case (Figure 9(a)), the thermal sensation gradually decreased to -2.5 as $T_{sk,m}$ decreased to 30.5 ºC during the first 30 minutes. Because of the heavy insulation, the change in $T_{sk,m}$ was slower than the change in the *TSV*. When the mean skin temperature fluctuated, the thermal sensation changed accordingly, which can also be observed in the mild case. At t = 35 minutes in Figure 9(b), the *TSV* dropped from -1.2 to -1.8, while $T_{sk,m}$ decreased from 32.1 to 31.7 ºC. At t = 45 minutes, when $T_{sk,m}$ rose to 32.2 ºC, the *TSV* increased to -0.9. The trend is also obvious in the hot case. As shown in Figure 9(c), the $T_{sk,m}$ of the subject increased to 35.3 ºC at t = 20 minutes, and the *TSV* of the subjects was 2.25. The warm feeling was gradually alleviated after the change rate of $T_{sk,m}$ reversed. At t = 45 minutes, the TSV decreased to 1.0, while $T_{sk,m}$ was still as high as 34.7 ºC.

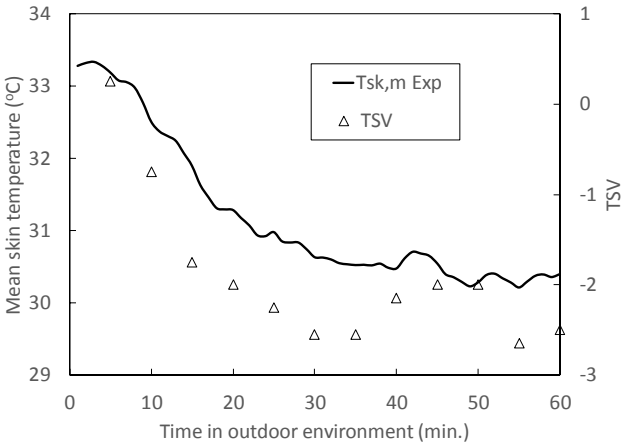

(a)

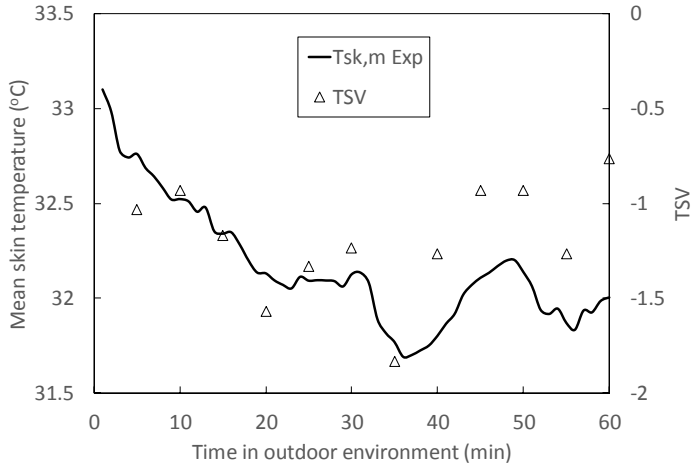

(b)

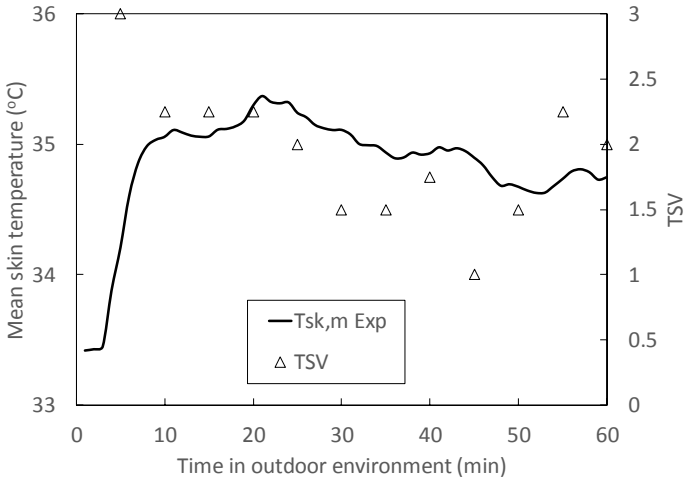

(c)

Figure 9. The measured $T_{sk,m}$ and the *TSV* reported by subjects in outdoor spaces: (a) cold case, (b) mild case, and (c) hot case.

As shown in Figure 9, small changes in the mean skin temperature could led to large changes in *TSV*. This is because of "alliesthesia." De Dear [26] defined alliesthesia as a phenomenon in which a pleasant feeling is evoked by the restoring of a regulated variable to its set-point. Alliesthesia is common in outdoor environments, where the skin temperature of the human body frequently deviates from the set point and the dynamic outdoor environment mediates the deviation. As a result, the alliesthesia effect is one of the reasons for the large discrepancy in outdoor thermal comfort found across different studies. Figure 9 showed that the alliesthesia effect exists at certain times. When pooling all the data obtained in the subject tests, there was hardly any correlations between the changes in

the skin temperature and the changes in *TSV*. In our subject tests, the outdoor thermal environment cannot be controlled. To further understand the alliesthesia effect, experiment under controlled thermal environment may be conducted.

Generally, the mean skin temperature and the thermal sensation correlated well with each other in the present study. Figure 10 shows the scatter plot between $T_{sk,m}$ and *TSV*. The correlation in Figure 10 is 0.72, which is reasonably high. Therefore, the mean skin temperature is a good predictor of thermal comfort.

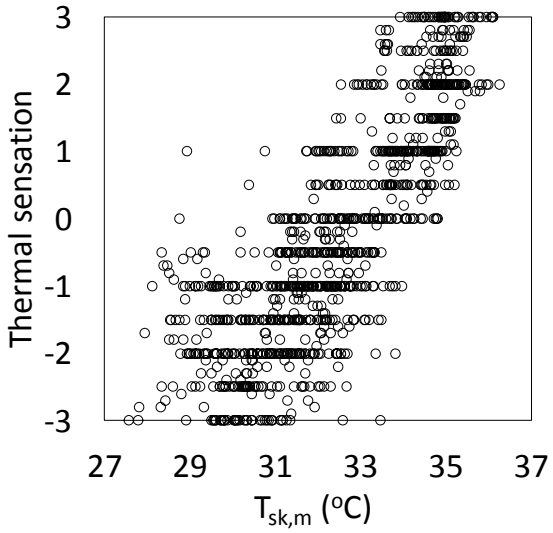

Figure 10. Scatter plot between $T_{sk,m}$ and *TSV*.

3.6.Local skin temperature

Please note that the above study used the mean skin temperature. Because of the different thermophysical properties of body segments and varying levels of clothing insulation on various body parts, the skin temperature was not the same at different body segments. The difference was more obvious in outdoor spaces because of the wide ranges of the thermal conditions.

Using the cold case as an example, Figure 11 compares the measured and modeled local skin temperature for subjects in the cold case. The temperature of the upper body segments, such as the abdomen, thorax, and arms, was almost constant because of the heavy insulation. For segments without clothing, such as the head, face, and hands, the temperature decreased rapidly. At the end of the test, the face had the lowest temperature of 19 ^{o}C, whereas the thorax temperature was 34.7 ^{o}C; the difference was 15.7 K. Note that the

temperature of the foot decreased by only 1.2 K, from 32.7 ºC to 31.5 ºC. This was probably due to the high heat generation in the feet when a subject remained in the standing position.

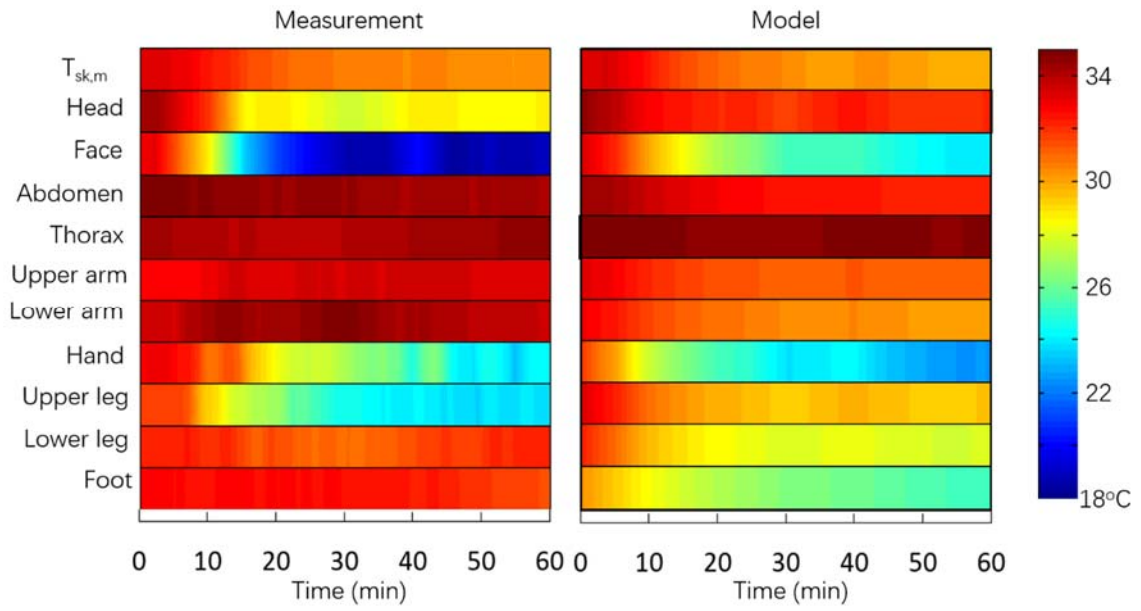

Figure 11. Comparison between the measured and predicted skin temperature at different body segments of the subjects in the cold case.

The model's prediction of the local skin temperature captured the general trend. For example, the model correctly predicted that the face temperature was the lowest. However, at the end of the test, the predicted face temperature was 5 *K* higher than the measured temperature. The deviation may have been due to inaccuracy in the local properties that were used, such as local clothing properties, local metabolic heat production values, and local counter-current heat exchange coefficients. A study by Vseela et al. [27] revealed that the use of different local properties can cause a 0.4–4.4 K difference in local skin temperature. Our model estimated the local clothing insulation by converting the whole-body clothing insulation of a clothing element to its local value [19], which was not sufficiently accurate. The local metabolic rate and the local counter-current heat exchange coefficient in our model were from empirical data provided by [25], who obtained some of the coefficients by a trial-and-error procedure that matched the predicted and measured skin temperatures.

In summary, local skin temperatures at different segments vary greatly and are harder

to predict than mean skin temperature. Although the results are not presented here, similar trends and prediction accuracy were found for the mild and hot cases. At some body segments, the measured and predicted skin temperature can differ greatly.

4. Discussion

As pointed out in previous studies [25,28], core temperature is an important physiological parameter that affects thermal comfort. Besides the thermoreceptors at skin, the thermoreceptors at body core also plays a crucial part in the integrated signals for thermoregulation. Core temperature is also central in the alliesthesia theory [26,29]. However, because of the large inter- and intra-personal variability of core temperature [28], we did not obtain this parameter.

Wind speed was measured by a vane anemometer or cup anemometer in our study. These two types of anemometer are easy to use outdoors, but they are not accurate when the wind speed is low. A more accurate instrument, such as an ultrasonic anemometer, should be used in the future.

The age of the subjects has a wide range from 19 to 59. Since the physiological conditions, such as heat generation and sweat excretion for various ages of people are different, potential inter-personal uncertainties might be introduced in the data.

Ideally, the long-wave radiation from the surroundings should be measured by six long wave infrared radiation pyrgeometer in orthogonal directions. This study used the method from RayMan software to estimate the long-wave radiation from the sky and the solid surfaces and distributed the long-wave radiation averagely on the human surface. This would inevitably introduce errors on the boundary conditions and the model calculation of skin temperature.

Most previous studies concerning outdoor thermal comfort used the field survey approach. The focus was on the relationship between the thermal environment and the thermal sensation. The skin temperature was not measured. This study obtained the skin temperature and used it as a bridge between the thermal environment and the thermal sensation. Instead of just collect one point of data in the previous field survey study, this investigation obtained the data during the entire exposure. This allowed us to study the dynamic part of thermal comfort.

5. Conclusions

This paper presented our study of dynamic thermal comfort in outdoor environments. With the use of human subjects, the investigation measured outdoor thermal environmental parameters, monitored the subjects' skin temperature at different body segments, and recorded the subjects' thermal sensation. A total of 26 subjects participated in our study, which generated 94 sets of data under different climatic conditions with outdoor air temperatures ranging from -0.1 to 35.0 ^{o}C. The following conclusions can be drawn from the study.

The outdoor measurements show that the wind speed and solar radiation fluctuated significantly during the tests, while the air temperature and relative humidity were relatively stable. The strong fluctuation in wind speed and solar radiation led to rapid changes in the convective and radiative thermal loads, which affected the mean skin temperature of the human subjects and the thermal sensation that they reported. The local skin temperature at the trunk in the cold conditions did not change much (remaining at around 34 ^{o}C) because of heavy insulation and large thermal capacity, while the face temperature decreased to as low as 19 ^{o}C.

This investigation developed a human heat transfer model that accounts for fluctuations in the outdoor thermal environment. The model considers short-wave and long-wave radiation in an outdoor space and includes transient heat transfer for clothing at different body segments. Comparisons between the skin temperatures predicted by the model and the corresponding measured data show that the model can predict the mean skin temperature reasonably well. However, the discrepancy between the predicted and measured local skin temperature can be as large as 6 K.

The study found a good correlation between the mean skin temperature and the thermal sensation reported by the human subjects in the cold and mild conditions. The correlation was not as good for the hot conditions because of the phenomenon of alliethesia. The mean skin temperature is a very important parameter for evaluating outdoor thermal comfort.

Acknowledgement

This research was partially supported by the national key project from the Ministry of Science and Technology, China, on "Green Buildings and Building Industrialization" through Grant No. 2016YFC0700500 and the China Scholarship Council (CSC).

References

[1] Population Reference Bureau. 2016 World Population Data Sheet. <http://www.prb.org/Publications/Datasheets/2016/2016-world-population-data-sheet.aspx >, 2016.

[2] T. Takano, N. Keiko, W. Masafumi, Urban residential environments and senior citizens' longevity in megacity areas: The importance of walkable green spaces, Journal of Epidemiology and Community Health 56(12) (2002) 913-918.

[3] J. Maas, S.M. van Dillen, R.A. Verheij, P.P. Groenewegen, Social contacts as a possible mechanism behind the relation between green space and health, Health and Place 15(2) (2009) 586-595.

[4] T.P. Lin, K.T. Tsai, C.C. Liao, Y.C. Huang, Effects of thermal comfort and adaptation on park attendance regarding different shading levels and activity types, Building and Environment 59 (2013) 599-611.

[5] M. Nikolopoulou, N. Baker, K. Steemers, Thermal comfort in outdoor urban spaces: Understanding the human parameter, Solar Energy 70(3) (2001) 227-235.

[6] M. Nikolopoulou, S. Lykoudis, Thermal comfort in outdoor urban spaces: Analysis across different European countries, Building and Environment 41(11) (2006) 1455-1470.

[7] S. Thorsson, M. Lindqvist, S. Lindqvist, Thermal bioclimatic conditions and patterns of behaviour in an urban park in Göteborg, Sweden, International Journal of Biometeorology 48(3) (2004) 149-156.

[8] S. Thorsson, T. Honjo, F. Lindberg, I. Eliasson, E.M. Lim, Thermal comfort and outdoor activity in Japanese urban public places, Environment and Behavior 39(5) (2007) 660-684.

[9] J. Spagnolo, R. de Dear, A field study of thermal comfort in outdoor and semi-outdoor environments in subtropical Sydney Australia, Building and Environment 38 (2003) 721-738.

[10] F. Aljawabra, M. Nikolopoulou, Outdoor thermal comfort in the hot arid climate: The effect of socio-economic background and cultural differences, 26th International Conference on Passive and Low Energy Architecture, Quebec City, Canada, 2009.

[11] D. Lai, D. Guo, Y. Hou, C. Lin, Q. Chen, Studies of outdoor thermal comfort in northern China, Building and Environment 77 (2014): 110-118.

[12] T.P. Lin, A. Matzarakis, Tourism climate and thermal comfort in Sun Moon Lake, Taiwan, International Journal of Biometeorology 52 (2008) 281-290.

[13] A. Matzarakis, H. Mayer, Another kind of environmental stress: Thermal stress, WHO News 18 (1996) 7-10.

[14] P. Höppe, Different aspects of assessing indoor and outdoor thermal comfort, Energy and Buildings 34(6) (2002) 661-665.

[15] G. Katavoutas, H.A. Flocas, A. Matzarakis, Dynamic modeling of human thermal comfort after the transition from an indoor to an outdoor hot environment, International Journal of Biometeorology 59(2) (2015) 205-216.

[16] A. Matzarakis, F. Rutz, H. Mayer, Modelling radiation fluxes in simple and complex environments: Basics of the RayMan model, International Journal of Biometeorology 54(2) (2010) 131-139.

[17] A. Matzarakis, F. Rutz, H. Mayer, Modelling radiation fluxes in simple and complex environments – Application of the RayMan model, International Journal of Biometeorology 51 (2007) 323–334.

[18] P. Bröde, D. Fiala, K. Błażejczyk, I. Holmér, G. Jendritzky, B. Kampmann, B. Tinz, G. Havenith, Deriving the operational procedure for the Universal Thermal Climate Index (UTCI), International Journal of Biometeorology 56(3) (2012) 481-494.

[19] D. Lai, Q. Chen, A two-dimensional model for calculating heat transfer in the human body in a transient and non-uniform thermal environment, Energy and Buildings 118 (2016) 114-122.

[20] K. Kubaha, D. Fiala, J. Toftum, A.H. Taki, Human projected area factors for detailed direct and diffuse solar radiation analysis, International Journal of Biometeorology 49(2) (2004) 113-129.

[21] T.P. Lin, K.T. Tsai, R.L. Hwang, A. Matzarakis, Quantification of the effect of thermal

indices and sky view factor on park attendance, Landscape and Urban Planning 107(2) (2012) 137-146.

[22] J. Monteith, M. Unsworth, Principles of Environmental Physics, Academic Press, Cambridge, U.S. 2007.

[23] M. Nikolopoulou, K. Steemers, Thermal comfort and psychological adaptation as a guide for designing urban spaces, Energy and Buildings 35(1) (2003) 95-101.

[24] B.W. Olesen, P.O. Fanger, The skin temperature distribution for resting man in comfort, Archives des Sciences Physiologiques 27(4) (1972) 385-393.

[25] D. Fiala, Dynamic Simulation of Human Heat Transfer and Thermal Comfort (PhD thesis), Leicester, UK: IESD, De Montfort University, 1998.

[26] R. de Dear, Revisiting an old hypothesis of human thermal perception: Alliesthesia, Building Research and Information 39(2) (2011) 108-117.

[27] S. Veselá, B.R.M. Kingma, A.J.H. Frijns, Local thermal sensation modelling–A review on the necessity and availability of local clothing properties and local metabolic heat production, Indoor Air (2016) doi:10.1111/ina.12324.

[28] H. Zhang, E. Arens, C. Huizenga, T, Han, Thermal sensation and comfort models for non-uniform and transient environments: Part I: Local sensation of individual body parts, Building and Environment 45(2) (2010): 380-388.

[29] T. Parkinson, R. de Dear, Thermal pleasure in built environments: Spatial alliesthesia from contact heating, Building Research and Information 44(3) (2016): 248–262.